Preparation and Properties of One Epoxy System Bearing Fluorene Moieties

Wenbin Liu,[1] Qihao Qiu,[2] Jun Wang,[1] Zichun Huo,[1] He Sun,[1] Xiuxia Zhao[1]

[1]*College of Materials Science and Chemical Engineering, Harbin Engineering University, Harbin 150001, China*
[2]*Ningbo Oceanking Chemical Development Company, Limited, Ningbo Chemical Industry Zone, Ningbo 315204, China*

Received 6 March 2008; accepted 20 January 2009
DOI 10.1002/app.30141
Published online 2 April 2009 in Wiley InterScience (www.interscience.wiley.com).

ABSTRACT: Diglycidyl ether of bisphenol fluorene (DGEBF) and 9,9-bis(4-aminophenyl) fluorene (BPF) were synthesized to introduce more aromatic structures into an epoxy system, and their chemical structures were characterized with Fourier transform infrared spectroscopy, NMR, and mass spectrometric analysis. The dynamic curing behavior of the DGEBF/BPF system was investigated with differential scanning calorimetry. DGEBF was cured with BPF, diaminodiphenylsulfone (DDS), and diaminodiphenylmethane (DDM), and E-44 (bisphenol A epoxide) was also cured with BPF for comparison. The thermal properties of the obtained polymers were evaluated with dynamic mechanical thermal analysis and thermogravimetric analysis. The cured DGEBF/BPF system showed a remarkably higher glass-transition temperature, better thermal stability and lower moisture absorption in comparison with the general bisphenol A epoxy resin/BPF system but approximated the heat resistance of the DGEBF/DDS and DGEBF/DDM systems. Such properties make this epoxy system very promising for heat-resistant applications. © 2009 Wiley Periodicals, Inc. J Appl Polym Sci 113: 1289–1297, 2009

Key words: resins; kinetics (polym.); thermal properties

INTRODUCTION

Epoxy resins have gained wide acceptance in applications involving advanced composite matrices, surface coatings, and semiconductor encapsulation because of their heat, solvent, and chemical resistance, good mechanical and electrical properties, and great adherence to many substrates.[1–3] In high-tech applications, however, epoxy resins with better heat and moisture resistance are required. For this reason, modifications of epoxy resins or curing agents, in both the backbone and pendant groups, have been continuously attempted to improve the thermal and physical properties of cured polymers.[4–6]

Many studies have been reported concerning improvements in the heat resistance of epoxy resins by increases in the crosslink density of a cured epoxy resin or the introduction of bulky structures such as dicyclopentadiene, biphenyl, naphthalene, and silsesquioxane.[7–10] Generally, the introduction of fluorene moieties into the epoxy chain is expected to greatly improve the thermal stability and moisture resistance of the polymer.[11] Korshak et al.[12] first synthesized diglycidyl ether of 9,9-bis(4-hydroxyphenyl) fluorene (BHPF) and found that its polymers cured with curing agents of diamine or anhydride had good heat resistance and high thermal stability. Lin et al.[13] and Chen et al.[14] reported several epoxy resins bearing fluorene structures and studied the effects of the chemical structure on the curing and thermal properties of the cured resins. Fluorene-based epoxy resins exhibited much higher glass-transition temperature (T_g), char yield (Y_c), and oxygen index values than a bisphenol A epoxy resin when trimethoxyboroxine was used as the curative. Dai et al.[15] prepared diglycidyl ether of BHPF by phase-transfer catalysis and intensively studied the curing and thermal degradation kinetics of a diglycidyl ether of bisphenol fluorene (DGEBF)/diaminodiphenylmethane (DDM) system. The results showed that DGEBF/DDM possessed thermal properties superior to those of diglycidyl ether of bisphenol A (DGEBA)/DDM. Fluorene-based epoxy resins have advantages of increased epoxy thermal stability and moisture resistance, but they are not satisfactory for some restricted applications because of lower T_g values and higher water uptake when they are cured with DDM or diaminodiphenylsulfone (DDS). Designing novel high-performance curing agents and modifying fluorene-based epoxides have been the trends of recent studies. Many new kinds of

Correspondence to: W. Liu (wjlwb@163.com).
Contract grant sponsor: Harbin Science & Technology Innovation Talents Fund; contract grant number: 2008RFXXG006.
Contract grant sponsor: Fundamental Research Fund of Harbin Engineering University; contract grant number: HEUF04070.

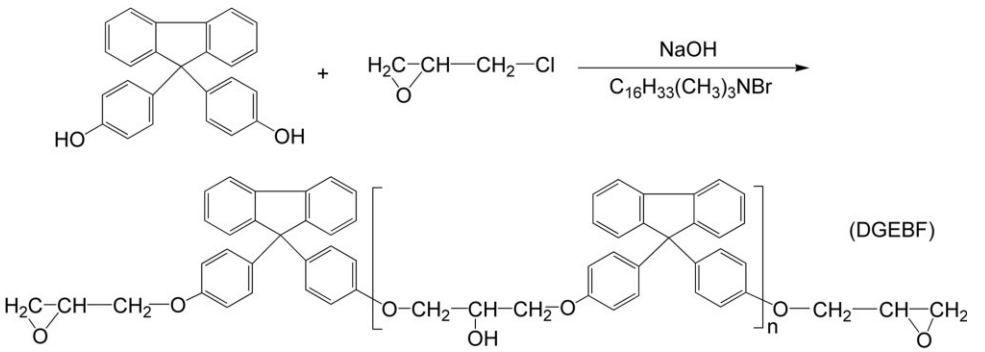

Scheme 1 Synthesis of DGEBF.

curing agents containing flexible or rigid hydrophobic groups or heterocyclic skeletons have been developed gradually.[16–18] However, descriptions of the curing kinetics and other fundamental issues about epoxy systems of DGEBF and a curing agent containing fluorene moieties have not been reported up to now.

In this study, DGEBF and 9,9-bis(4-aminophenyl) fluorene (BPF) were synthesized and characterized with IR, NMR, and mass spectrometry (MS). The curing kinetics of DGEBF/BPF were studied with dynamic differential scanning calorimetry (DSC) and simulated with Kissinger's method, and the thermal properties of the cured polymers were investigated with dynamic mechanical thermal analysis and thermogravimetric analysis (TGA).

EXPERIMENTAL

Materials

BHPF (99.0%) was synthesized according to Liu et al.[19] Fluorenone, epichlorohydrin (ECH), and hexadecyl trimethyl ammonium bromide (HTAB) were obtained from Beijing Chemical Co. (Beijing, China). Methylsulfonic acid was purchased from Sinopharm Group Chemical Reagent Co., Ltd. (Shanghai, China). Bisphenol A epoxy resin (epoxy equivalent weight = 227 g/equiv; commercial code E-44) was obtained from Wuxi Resin Co. (Wuxi, China). All solvents and other chemicals were reagent-grade or better and were used without further purification.

Synthesis of DGEBF

DGEBF was synthesized from BHPF and ECH by a previously reported method[15] (yield = 93.6%; mp = 108–114°C). The synthetic route is shown in Scheme 1.

IR (KBr, cm^{-1}): 2930 (—CH_2O—), 1240, 1028 (C—O—C), 911 (oxirane). ^{1}H-NMR [400 MHz, chloroform-*d* ($CDCl_3$), δ]: 6.790–7.774 (m, 16H, ArH), 4.144–4.180 (dd, J = 11.2 Hz, J = 3.2 Hz, CH_2 of glycidyl, 2H), 3.887–3.929 (dd, J = 11.2 Hz, J = 5.6 Hz, CH_2 of glycidyl, 2H), 3.309–3.343 (m, CH of epoxy, 2H), 2.878–2.900 (t, J = 4.4 Hz, CH_2 of epoxy, 2H), 2.733–2.752 (dd, J = 4.8 Hz, J = 2.8 Hz, CH_2 of epoxy, 4H), 1.60 (s, 2H, OH).

Synthesis of BPF

Fluorenone (18.0 g, 0.10 mol), aniline (74.6 g, 0.80 mol), and methylsulfonic acid (4.80 g, 0.050 mol) were added to a 250-mL, three-necked, round-bottom flask equipped with a heating mantle, a magnetic stirrer, a reflux condenser, a thermometer, and a nitrogen inlet. A stream of nitrogen was introduced, and the mixture was heated to 145–150°C for 10 h with stirring. The water that formed in the condensation reaction was retained in the flask throughout the reaction. The flask was cooled, and its contents were poured into 300 mL of ethanol containing 5.0 g of triethylamine. The off-white precipitated product was filtered and washed with an aqueous ethanol solution until the effluent was colorless. The product was then dried *in vacuo*, recrystallized from toluene, and dried *in vacuo* at 100°C for 24 h. A white solid of 20.4 g was obtained [yield = 58.6%; purity HPLC = 99.4%; mp = 237–238°C]. The reaction equation in shown in Scheme 2.

IR (KBr, cm^{-1}): 3375, 3511 (N—H), 1178 (C—N), 826 (C—H_{Ar}). ^{1}H-NMR (400 MHz, $CDCl_3$, δ): 6.540–7.771 (m, 16H, ArH), 3.550 (s, 4H, NH). ^{13}C-NMR (100 MHz, $CDCl_3$, δ): 152.25 (2, ArC of C—N), 144.82, 139.95, 136.17 (6, ArC), 129.09 (4, meta =C of aniline), 127.58, 127.08, 126.03 (6, ArC), 120.01 (2, ArC), 114.88 (4, ortho =C of aniline), 64.16 (quaternary carbon). MS (m/z): calcd for $C_{25}H_{20}N_2$, 348.44; found, 349.5 $[M+H]^+$. ANAL. calcd for $C_{25}H_{20}N_2$: C,

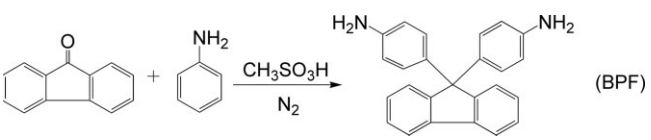

Scheme 2 Synthesis of BPF.

86.17%; H, 5.79%; N, 8.04%. Found: C, 86.18%; H, 5.79%; N, 8.03%.

Resin casting preparation

The epoxy resins were initially heated up to 125–130°C and degasified for 10–15 min *in vacuo*. A theoretical mass stoichiometric proportion of the curing agent was added to the epoxy resins, and the contents were thoroughly mixed; the treated epoxy resins were then cast into a preheated steel mold (130–135°C) coated with a mold-release agent. Deaeration was carefully conducted again, and the resins were cured in sheet molds via heating in an air-circulated oven with a programmed curing process. The cured resins were allowed to cool to the ambient temperature and then were removed from the oven and cut into a suitable size.

Characterization

Fourier transform infrared (FTIR) spectra were recorded on a Nicolet Avatar 370 FTIR spectrometer (Nicolet, USA) in the range of 4000–500 cm^{-1}. The samples were milled with potassium bromide, and the powder of the mixture was then pressed into disks for FTIR measurements. ^{1}H-NMR and ^{13}C-NMR characterizations were performed on a Bruker Avance-400 NMR spectrometer (Bruker Brospin, USA) with $CDCl_3$ as the solvent and tetramethylsilane as the internal standard. Mass spectrographic analyses were performed on an Agilent 1100LC mass spectrometer (Agilent Technologies, USA). Elemental analyses were performed on an Italy EA 1112 elemental analyzer (ThermoQuest, Milan, Italy) for C, H, and N determination. DSC measurements were evaluated on a Netzsch 204C differential scanning calorimeter (Netzsch Instruments, Savaria, Germany) under a constant flow of nitrogen at 20 mL/min. The instrument was calibrated with a high-purity indium standard, and α-Al_2O_3 was used as the reference material. The DGEBF and curing agent reactants were mixed homogeneously in a 1 : 1 molar equivalent ratio. About 10 mg of a sample was weighed into a hermetic aluminum sample pan at 25°C; it was then sealed, and the sample was tested immediately. The dynamic scanning experiments ranged from 25 to 300°C at heating rates of 5, 10, 15, and 20°C/min. TGA was performed with a TA Q50 (TA Instruments, New Castle, DE) at a heating rate of 10°C/min from 25 to 700°C under a nitrogen atmosphere at a flow rate of 60 mL/min. The dynamic mechanical thermal properties of the epoxy thermosets were carried out with a TA Q800 dynamic mechanical analyzer (TA Instruments). The rectangular samples (20 mm × 5 mm × 2 mm) were loaded in a single-cantilever mode with a temperature ramp of 3°C/min from 30 to 300°C at a frequency of 1 Hz under an air atmosphere. Moisture absorption was determined as follows: the rectangular samples (20 mm × 5 mm × 2 mm) were dried *in vacuo* at 100°C for 12 h, cooled to room temperature, weighed, placed in 100°C water for a period of time, and reweighed. The moisture absorption was calculated as the weight gain percentage:

$$\text{Moisture absorption}(\%) = (W/W_o - 1) \times 100\%$$

where W is the weight of the sample after it was dipped in 100°C water for a period of time and W_o is the weight of the sample after it was placed in a vacuum oven for 12 h.

RESULTS AND DISCUSSION

Synthesis and characterization

DGEBF was synthesized from BHPF and ECH by phase-transfer catalysis according to the methods described by Dai et al.[15] In their report, tetraethyl ammonium bromide was used as the phase-transfer catalyst in the etherification of BHPF with ECH. In our experiment, we used HTAB as the phase-transfer catalyst, and the mixed solvent consisted of ethanol and dioxane as a carrier to remove water produced in the ring-closing reaction. It was finally found that HTAB could substitute for tetraethyl ammonium bromide in the etherification step without any loss of yield via the combined use of the mixed solvent. Figure 1 shows the FTIR spectra of DGEBF and BPF. In comparison with the FTIR spectra of BHPF,[19] four new absorption peaks appeared in the FTIR spectra of DGEBF: the absorption peak at 2930 cm^{-1} indicated an O—CH_2 stretching vibration,

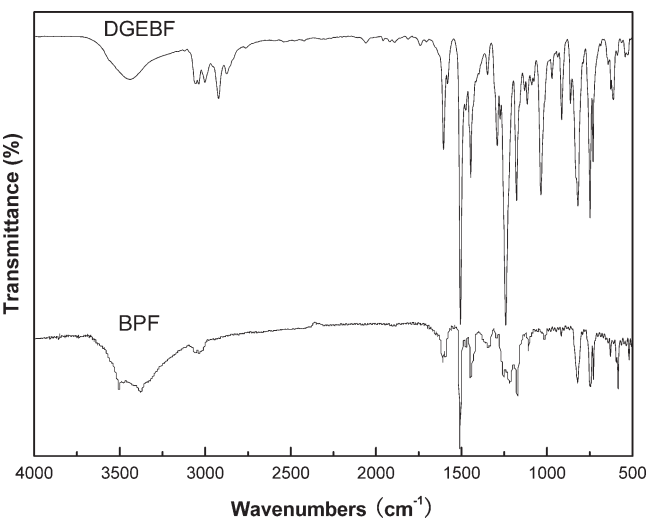

Figure 1 IR spectra of DGEBF and BPF.

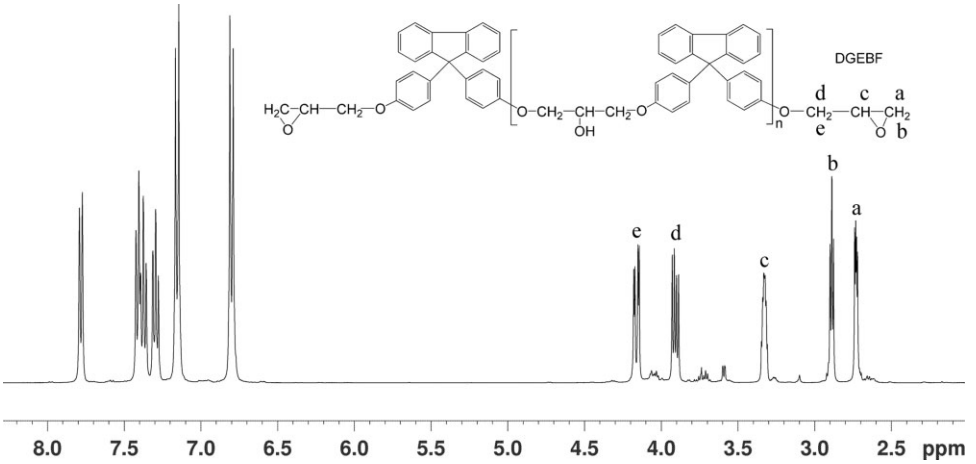

Figure 2 ^{1}H-NMR spectrum of DGEBF.

the peaks appearing at about 1240 and 1028 cm^{-1} could be assigned to the C—O—C stretching vibration, and the band observed at 914 cm^{-1} was attributed to the stretching vibration of the oxirane ring. These four characteristic peaks suggested the occurrence of etherification between BHPF and ECH and also confirmed the chemical structure of the synthesized resin. The ^{1}H-NMR spectrum (δ) for DGEBF is shown in Figure 2. The chemical shifts corresponding to the protons of the glycidyl ether group were found at 2.733–4.180 (10H). Chemical shifts observed at 6.790–7.774 (16H) were assigned to aromatic protons, and those at 6.790–6.812 (t, 4H) and 7.144–7.167 (t, 4H) corresponded to ortho protons and meta protons of the phenolic hydroxyl group, respectively.[15,20,21] The epoxy value, determined by the HCl/acetone titration method, was 0.40–0.41 mol/100 g in terms of the GB-1677-81 standard method (China).

The structure of BPF was confirmed with FTIR, ^{1}H-NMR, ^{13}C-NMR, and MS. The IR spectrum (Fig. 1) exhibited characteristic primary amine absorption at 3375 and 3511 cm^{-1} and para-disubstituted phenylene absorption at 826 cm^{-1}. The ^{1}H-NMR and ^{13}C-NMR spectra for BPF are shown in Figures 3 and 4, respectively. One broad single chemical shift attributed to four hydroxyl protons of primary amine was observed at 3.550 ppm (4H). The chemical shifts corresponding to the protons of ortho and meta hydroxyl protons were observed at 6.540–6.562 (4H) and 7.015–7.036 ppm (4H), respectively. Furthermore, the ^{13}C-NMR spectrum of BPF exhibited a single peak at 64.16 (C_a), which indicated the existence of a quaternary carbon atom. The ^{1}H-NMR spectra and characteristic bands in the IR spectra were in agreement with the results reported by Hua et al.[22] and Liu et al.,[23] identifying the structure of BPF. In the mass spectrum of BPF,

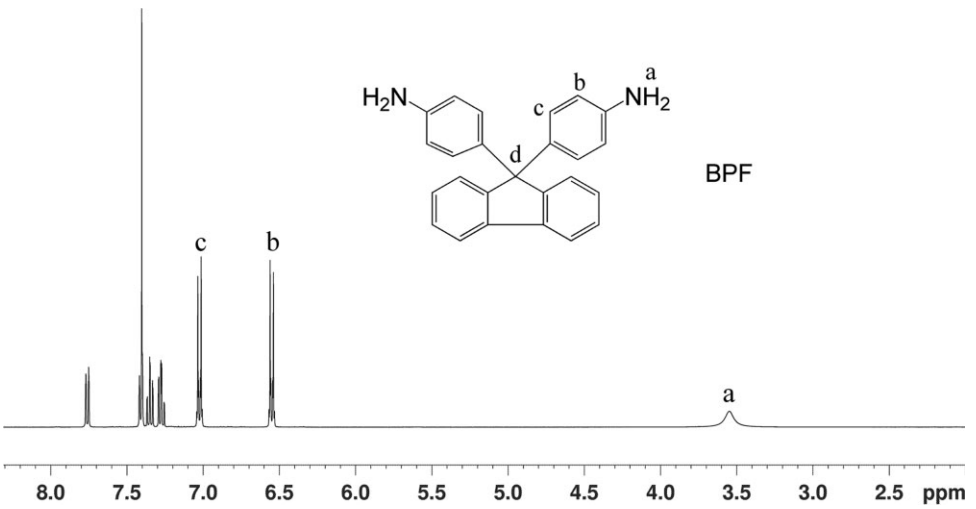

Figure 3 ^{1}H-NMR spectrum of BPF.

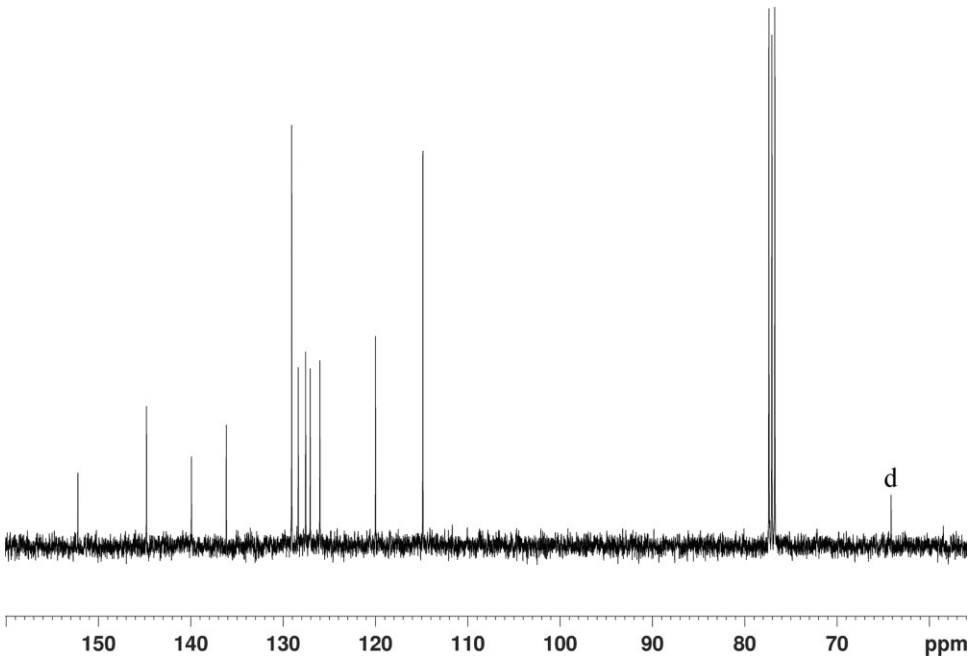

Figure 4 ^{13}C-NMR spectrum of BPF.

a peak of $m/z = 349.5$ ($[M+H]^+$) also supported the proposed structure.

From the viewpoint of the molecular structure, DGEBF and BPF contain a fairly large number of aromatic rings; this ensures thermal stability and flame retardancy as well.[14]

Curing behaviors of DGEBF/BPF

The curing reaction of DGEBF/BPF was studied with nonisothermal DSC methods. Figure 5 shows dynamic DSC thermograms of the DGEBF/BPF curing reaction at heating rates of 5, 10, 15, and 20°C/min. The exothermic peak temperature (T_p) of the curing curves shifted to higher temperatures with the increasing heating rate.

To evaluate the kinetic parameters of the DGEBF/BPF system, Kissinger's method[24] was applied to calculate the activation energy (E_a) because it is a very simple way of dealing with the dynamic curing process of an epoxy–amine system. The kinetic parameters can be obtained with Kissinger's method without the need of any assumption about a conversion-dependent equation.[25]

Kissinger's equation can be expressed as follows:

$$-\ln\left(\frac{\beta}{T_p^2}\right) = \frac{E_a}{RT_p} - \ln\frac{AR}{E_a} \quad (1)$$

where β is the heating rate, A is the Arrhenius constant, and R is the ideal gas constant. Therefore, E_a could be obtained from the slope of a plot of $\ln(\beta/T_p^2)$ versus $1/T_p$ (Fig. 6). The calculated value of E_a was 57.66 kJ/mol, and the linear correlation coefficient was 0.996. According to the aforementioned method, the E_a value of E-44/BPF was 53.08 kJ/mol.

Furthermore, the curing reaction order (n) can be obtained when the Crane method,[26] as shown in eq. (2), is applied:

$$\frac{d(\ln\beta)}{d(1/T_p)} = -\left[\frac{E_{a,k}}{nR} + 2T_p\right] \quad (2)$$

where $E_{a,k}$ is the activity energy calculated with Kissinger's method. n, obtained from the slope of a plot of ln(β) versus $1/T_p$ (Fig. 6), was 0.89, and the linear correlation coefficient was 0.997.

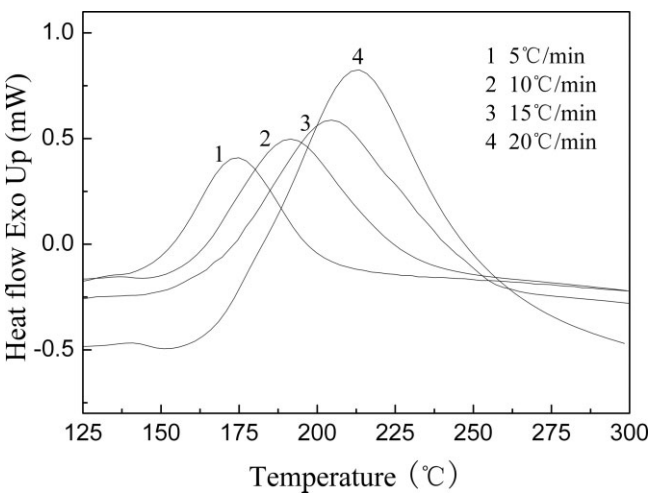

Figure 5 Dynamic DSC thermograms of DGEBF/BPF curing reactions at heating rates of 5, 10, 15, and 20°C/min under nitrogen.

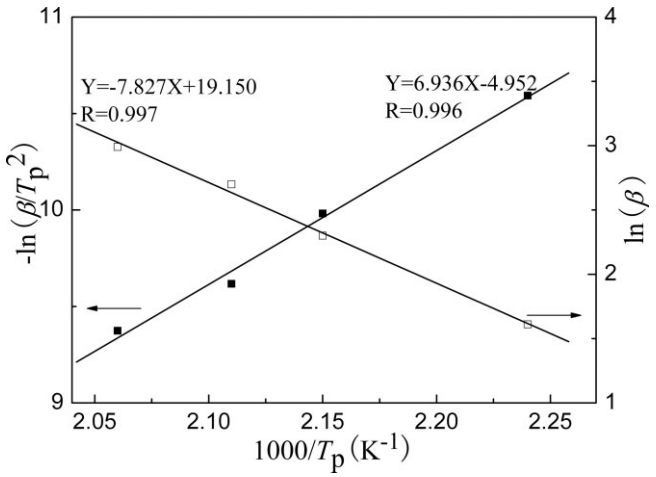

Figure 6 Curing kinetic analysis and calculation of the curing E_a values for DGEBF/BPF.

According to Kissinger's method, A, which can be calculated with the following equation, was 9.699×10^5:

$$A = \frac{\beta E_a \exp[E_a/RT_p]}{RT_p^2} \tag{3}$$

Thus, the curing kinetic model can be expressed as follows:

$$\frac{d\alpha}{dt} = 9.699 \times 10^5 \exp\left(-\frac{57660}{RT}\right)(1-\alpha)^{0.889} \tag{4}$$

where α is the degree of curing.

The calculated value of E_a for the DGEBF/BPF system from Kissinger's method was higher than the result for the DGEBF/DDM (51.65 kJ/mol in ref. 16) and E-44/BPF systems but was lower than that for the DGEBF/DDS system (63.86 kJ/mol).[27] This indicated that BPF had lower reactivity toward epoxy groups because of the steric hindrance of fluorene moieties, and this might be useful in tailoring the processing factors in the manufacturing process. The reactivity of DDS toward the epoxy resin was the lowest of all the curing agents because the sulfone group in DDS is a strong electron-withdrawing group.[28]

The starting temperature of the exothermic reaction corresponded to the initial crosslinking temperature (T_i). T_p was related to the curing peak temperature. The postcuring temperature (T_f) was associated with the terminal temperature of the exothermic reaction.[15] T_i, T_p, and T_f of exothermic curves obtained from DSC at different heating rates were plotted against the heating rates and extrapolated to zero heating rates (Fig. 7). The values of the extrapolated temperatures at zero heating rates could be used for curing conditions. As an example of a DGEBF/BPF system, we can see from Figure 6 that the T_i, T_p, and T_f values extrapolated to zero heating rates were 146.5, 164.0, and 188.4°C, respectively. According to these parameters, we could approximately determine the curing conditions of the DGEBF/BPF system as 150°C for 1 h, 180°C for 3 h, and 200°C for 1 h. The curing conditions of the other system were determined with the same method.

Dynamic mechanical thermal analysis

Dynamic mechanical observations were carried out to analyze the dynamic elastic (or storage) modulus and the occurrence of glass transitions for different cured epoxy systems. Temperature-dependence curves of the storage modulus and tan δ values of different cured polymers are shown in Figure 8(a,b), respectively. All the fluorene epoxides possessed higher storage moduli than the E-44/BPF system in both glassy and rubbery regions. This could obviously be the contribution of the rigid fluorene moieties. However, the modulus might have been affected by the crosslink density of the epoxy resins. The crosslink density (ρ) was determined with the following equation:[29,30]

$$\rho = E/3RT \tag{5}$$

where E is the storage modulus at $T_g + 50$°C and T is the absolute temperature at $T_g + 50$°C. The T_g, E, and crosslink density values of different epoxy thermosets are summarized in Table I.

As shown in Table I, the modulus of the DGEBF/BPF system (1785 MPa) was higher than that of the DGEBF/DDS (1712 MPa) and DGEBF/DDM (1366 MPa) systems in the glassy region but lower in the rubbery region, such as $T_g + 50$°C. It is possible that the rigid fluorene ring made a leading contribution to the rigidity of the epoxy thermosets in the glassy

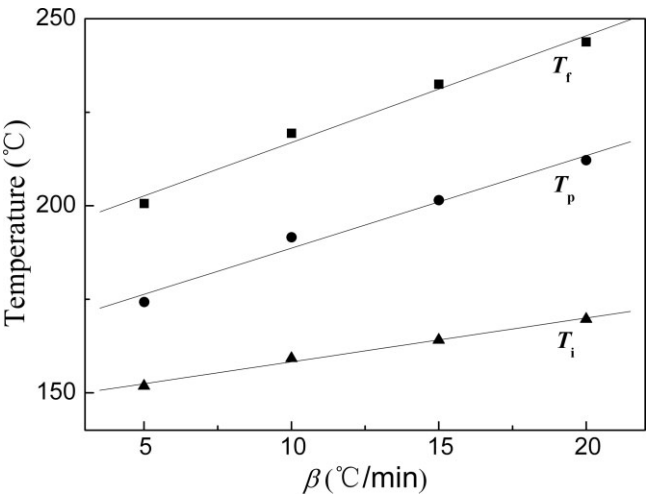

Figure 7 T_f, T_i, and T_p values for DGEBF/BPF.

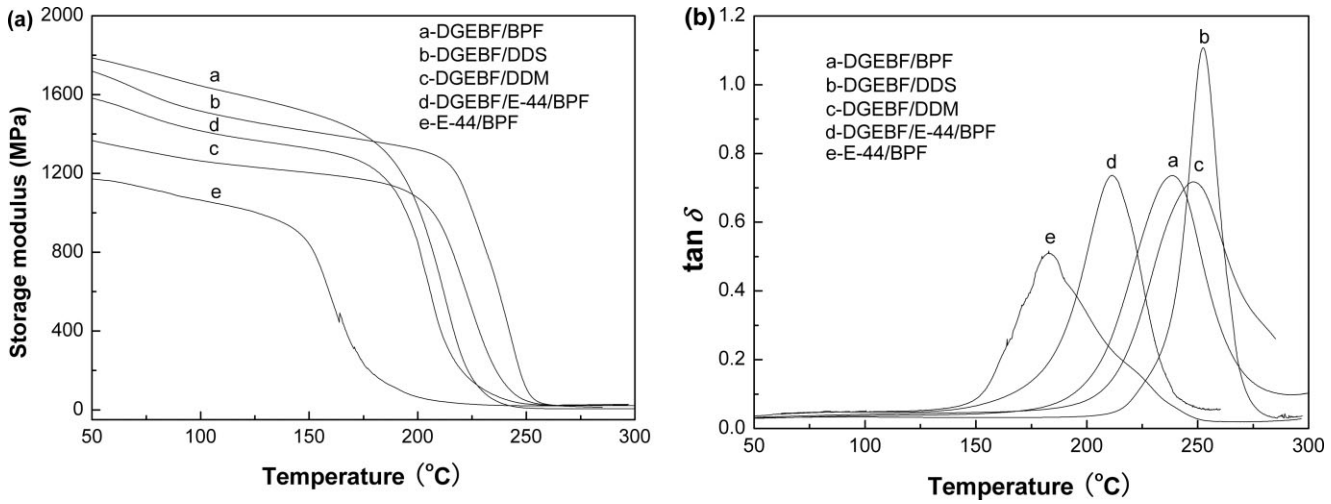

Figure 8 Temperature-dependence curves of (a) the storage modulus and (b) tan δ for cured epoxy thermosets.

state. Compared with DGEBA, DGEBF has a structure in which a bulky fluorene unit protrudes vertically from the polymer main chain. This chemical structure of four phenyl rings connected to a quaternary carbon leads to severe rotational hindrance of the phenyl groups.[30] Therefore, the stiff, bulky cardo moiety would arise from the higher rigidity of the fluorene skeleton in the chain backbone, and the modulus of the DGEBF/BPF system was much higher than that of the DGEBA/BPF system in the glassy state. For the different curing agents, the modulus order was BPF > DDS > DDM in the glassy state. The higher modulus of the BPF system versus that of the DDS and DDM systems was ascribed to the rigidity of the cured epoxy resin due to the steric hindrance of fluorene moieties. However, in the rubbery state, the storage modulus decreased with the decline of the crosslink density; it was deduced that the rigidity of the cured resin was dominated by the crosslink density.

The peak temperature of tan δ was taken to be T_g. Figure 8(b) and Table I indicate that T_g of the cured polymer from the DGEBF/BPF system was 238.5°C and therefore higher than the T_g values of E-44/BPF, DGEBA/DDM,[15,31] and DGEBA/DDS[32] (183.0, 167.0–194.8, and 200.4°C, respectively) and close to those of the cured DGEBF/DDM and DGEBF/DDS polymers (248.0 and 252.5°C, respectively). T_g is affected by both the crosslink density and the backbone rigidity of the epoxy monomer. The obvious difference in the T_g values of the DGEBF/BPF and E-44/BPF polymers can be attributed to the chemical structures of the chains; the bulky fluorene moiety would restrain the internal rotations and thermal motion of the polymer segments.[23] As a result, the T_g value for cured DGEBF/BPF was about 55°C higher than that of DGEBA/BPF. However, for the systems of DGEBF cured with BPF, DDS, and DDM, the results showed that the T_g values of the epoxy thermoset, which were about 50°C higher than those of the corresponding DGEBA system, depended on the degree of crosslinking and increased with an increase in the crosslink density. For the DGEBF/E-44/BPF blend system (mass ratio of DGEBF to E-44 was 1:1), the modulus and T_g of the cured resin were higher than those of the E-44/BPF system

TABLE I
Dynamic Mechanical Analysis of the Cured Resins

Sample	T_g (°C)	Storage modulus (MPa)		$\rho \times 10^{-3}$ (mol/cm^3)
		50°C	T_g + 50°C	
DGEBF/BPF	238.5	1785	5.152	0.37
DGEBF/DDS[a]	252.5	1712	27.11	1.89
DGEBF/DDM[b]	248.0	1366	12.54	0.88
DGEBF/E-44/BPF[a]	211.7	1581	22.37	1.68
E-44/BPF[a]	183.0	1171	23.82	1.89

[a] The curing process: 150°C/1 h + 180°C/3 h + 200°C/2 h.
[b] The curing process: 120°C/2 h + 150°C/3 h + 180°C/2 h.

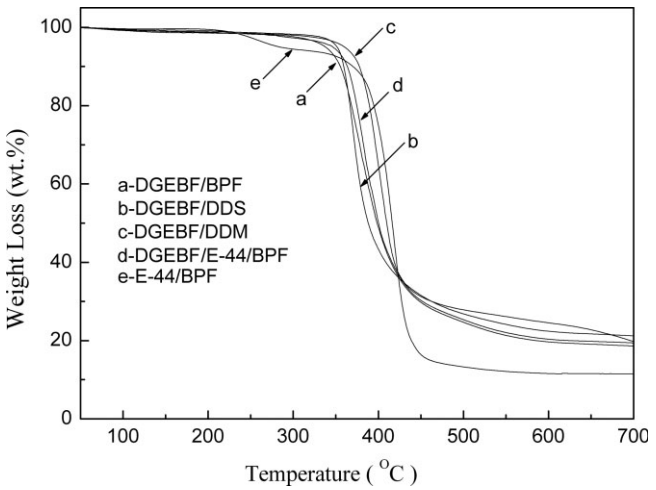

Figure 9 TG thermograms of cured polymers.

because of the introduction of rigid fluorene groups into the backbone of the epoxy network.[33] This indicated that both the chemical structure and crosslink density of the epoxy resin played predominant roles in raising the modulus and T_g of the blend resin system.

TGA

Thermal stability was evaluated by TGA under a nitrogen atmosphere, and thermal property parameters of different epoxy thermosets are shown in Figure 9 and Table II.

The temperature corresponding to 5% weight loss ($T_{d,5\%}$) was taken as an index of thermal stability. The $T_{d,5\%}$ and Y_c values of the DGEBF system were much higher than those of DGEBA/BPF, and the cured DGEBF/DDS polymer exhibited better heat resistance than other cured epoxy systems. This result indicates that the introduction of the fluorene skeleton into the epoxy monomers improved the inherent thermal stability of the thermosets dramatically. Similar to the aforementioned dynamic mechanical thermal analysis measurement, the thermal stability was also controlled by two factors: the fluorene content and the crosslink density. The introduction of a rigid fluorene structure into the crosslink network could enhance internal rotation resistance stress and restrain the thermal movements and rotation of polymer chains,[15] but it could also induce a decrease in the crosslink density and a reduction of ductility. When the content of rigid segments was lower, the heat resistance of the system was mainly controlled by the content of fluorene moieties, whereas when the content of rigid fluorene was higher, a decreased crosslinking degree was caused, restricting further improvement in the thermal stability of the cured

TABLE II
Thermal Stability Parameters for the Cured Polymers

Sample	$T_{d,5\%}$ (°C)	$T_{d,10\%}$ (°C)	Y_c (%)
DGEBF/BPF	337.4	355.3	18.59
DGEBF/DDS	357.3	377.7	19.74
DGEBF/DDM	349.6	359.4	21.22
DGEBF/E-44/BPF	343.0	363.9	19.40
E-44/BPF	283.5	364.2	11.50

$T_{d,10\%}$ = temperature corresponding to 10% weight loss; Y_c = char yield at 700°C under N_2.

polymers. The DGEBF/DDM system possessed the highest Y_c value, and this might also have been induced by a higher crosslink density.

Moisture absorption

In practical usage, absorbed moisture was found to plasticize the epoxy resin, causing a lowering of T_g and in turn affecting the mechanical properties.[34] The moisture absorption measurements are listed in Table III. As shown in Table III, all cured epoxy resins bearing fluorene moieties, especially the DGEBF/BPF system, possessed better moisture resistance than those of neat bisphenol A epoxide (the water uptake values of DGEBA/DDS[35] and DGEBA/DDM[36] at equilibrium are 4.01 and 3.0%, respectively) and other epoxides (tetraglycidyl methylene dianiline epoxy/DDS, 8.92%;[35] tetramethyl biphenol epoxy/DDM, 2.40%, 24 h; tetramethyl biphenol/DDS, 2.90%, 24 h[28]). It seems that the hydrophobic fluorene moieties were responsible for the lower moisture absorption. During the curing process, hydrophilic hydroxyl groups, major reasons for the raised moisture absorption, were generated via the ring opening of epoxy groups.[30,37] The average volume of the fluorene ring was larger than that of the methyl group in bisphenol A epoxide, and it induced a decreased crosslink density in the network of cured polymers, which produced fewer hydroxyl groups because of the reduced ring opening of oxirane, thus leading to higher hydrophobicity of the system. In addition, the combination of fluorenyl moieties, which have more phenyl groups than

TABLE III
Moisture Absorption of the Cured Polymers

Sample	Water uptake (%)				
	12 h	24 h	36 h	48 h	72 h
DGEBF/BPF	1.53	1.72	1.79	1.85	1.89
DGEBF/DDM	1.54	1.69	1.77	1.96	2.30
DGEBF/DDS	1.70	1.84	1.98	2.18	2.46
E-44/DGEBF/BPF	1.38	1.56	1.69	1.91	2.04
E-44/BPF	1.39	1.59	1.69	1.86	2.12

conventional DGEBA or DDS and DDM, decreased the polarity of the polymer backbone and could further depress the water absorption.[38] Therefore, the DGEBF/BPF curing system showed remarkably lower water absorption in comparison with the other systems. For the blend systems, the incorporation of DGEBF, with its lower crosslink density and polarity in comparison with neat DGEBA, could effectively improve moisture resistance.

CONCLUSIONS

In this study, a novel epoxy system was prepared from DGEBF and BPF. With the introduction of massive fluorene moieties, the cured polymer exhibited a higher T_g value, better thermal stability, and lower moisture absorption than a bisphenol A epoxy resin. These pronouncedly good properties make it an attractive candidate for electronic encapsulation applications and composite matrices.

References

1. Blanco, I.; Cicala, G.; Costa, M.; Recca, A. J Appl Polym Sci 2006, 100, 4880.
2. Ho, T. H.; Leu, T. S.; Sun, Y. M.; Shieh, J. Y. Polym Degrad Stab 2006, 91, 2347.
3. Ren, S. P.; Liang, L. Y.; Lan, Y. X.; Lu, M. G. J Appl Polym Sci 2007, 106, 2917.
4. Liu, G. D.; Gao, J. G.; Song, L. L. Macromol Chem Phys 2006, 207, 2222.
5. Xu, K.; Chen, M. C.; Zhang, K.; Hu, J. W. Polymer 2004, 45, 1133.
6. Zhang, X. H.; Chen, S.; Min, Y. Q. Polymer 2006, 47, 1785.
7. Duan, Y. F.; Liu, T. M.; Cheng, K. C.; Su, W. F. Polym Degrad Stab 2004, 84, 305.
8. Teo, J. K. H.; Teo, K. C.; Pan, B.; Xiao, Y.; Lu, X. Polymer 2007, 48, 5671.
9. Lee, J. Y.; Shim, M. J.; Kim, S. W. J Appl Polym Sci 2002, 83, 2419.
10. Lin, C. H.; Chiang, J. C.; Wang, C. S. J Appl Polym Sci 2003, 88, 2607.
11. Lin, S. C.; Pearce, E. M. J Polym Sci Part A: Polym Chem 1979, 17, 3095.
12. Korshak, V. V.; Solovèva, L. K.; Kamenskh, I. V. Vysokomol Soedin 1971, 13, 150.
13. Lin, S. C.; Bulkin, B. J.; Pearce, E. M. J Polym Sci Polym Chem Ed 1979, 17, 3121.
14. Chen, C. S.; Bulkin, B. J.; Pearce, E. M. J Appl Polym Sci 1982, 27, 3289.
15. Dai, Z.; Li, Y. F.; Yang, S. G. J Appl Polym Sci 2007, 106, 1476.
16. Ren, H.; Sun, J. Z.; Wu, B. J.; Zhou, Q. Y. Chin J Chem Eng 2007, 15, 127.
17. Rwei, S. P.; Cheng, C. Y.; Liou, G. S. Polym Eng Sci 2005, 45, 478.
18. Srividhya, M.; Lakshmi, M. S.; Reddy, B. S. R. Macromol Chem Phys 2005, 206, 2501.
19. Liu, W.; Wang, J.; Qiu, Q. H.; Ji, L.; Wang, C. Y.; Zhang, M. L. Pigm Resin Technol 2008, 37, 9.
20. Liu, F.; He, J. W.; Lin, Z. M.; Ling, J. Q.; Jia, D. M. Molecules 2006, 11, 953.
21. Liu, W. B.; Wang, J.; Qiu, Q. H.; Zhang, M. L. Pigm Resin Technol 2008, 37, 389.
22. Hua, Z. Q.; Wang, M. H.; Li, S. J.; Liu, X. Y.; Wu, J. H. Polymer 2005, 46, 5278.
23. Liu, W. B.; Qiu, Q. H.; Wang, J.; Huo, Z. C.; Sun, H. Polymer 2008, 49, 4399.
24. Kissinger, H. E. Anal Chem 1957, 29, 1072.
25. López, J.; López-Bueno, I.; Nogueira, P.; Ramírez, C.; Abad, M. J.; Barral, L.; Cano, J. Polymer 2001, 42, 1669.
26. Crane, L. W.; Dynes, P. J.; Kaelble, D. H. J Polym Sci Polym Lett Ed 1973, 11, 533.
27. Niu, H. X.; Zhou, T.; Zhang, A. M.; Zhang, H.; Tang, G. B.; Ren, L. B. J Funct Polym 2007, 19, 358.
28. Lin, C. H.; Huang, J. M.; Wang, C. S. Polymer 2002, 43, 2959.
29. Xie, M. R.; Wang, Z. G.; Zhao, Y. F. J Polym Sci Part A: Polym Chem 2001, 39, 2799.
30. Kazama, S.; Sakashita, M. J Membr Sci 2004, 243, 59.
31. Pethrick, R. A.; Dejean, R.; Marie, F.; Hollins, E. A.; McEwan, L.; McNairney, S. Int J Polym Mater 1998, 40, 197.
32. Pan, G. Y.; Du, Z. J.; Zhang, C.; Li, C. J.; Yang, X. P.; Li, H. Q. Polymer 2007, 48, 3686.
33. Ren, H.; Sun, J. Z.; Wu, B. J.; Zhou, Q. Y. Polymer 2006, 47, 8309.
34. Prolongo, S. G.; Rosario, G. D.; Ureña, A. Int J Adhes Adhes 2006, 26, 125.
35. St. Clair, A. K.; Stoakley, D. M.; St. Clair, T. L. U.S. Pat 4,510,277 (1985).
36. Chateauminois, A.; Sauvant, V.; Halary, J. L. Polym Int 2003, 52, 507.
37. Swier, S.; Assche, G. V.; Vuchelen, W.; Bruno, V. M. Macromolecules 2005, 38, 2281.
38. Xu, K.; Chen, M. C.; Zhang, K.; Hu, J. W. Polymer 2004, 45, 1133.